Linear and Nonlinear Elastic Behaviors of Star Polymers

Satoru Masatsuji, Natsuko Nakagawa, and Kaoru Ohno*

Department of Physics, Yokohama National University, 79-5 Tokiwadai, Hodogaya, Yokohama 240-8501, Japan

Received August 24, 2008; Revised Manuscript Received January 7, 2009

ABSTRACT: In this paper, we investigate the elastic behavior of M-arm star polymers in good solvents under an external force X exerted on each end of the arms in the x direction. In the region of small X, there is a slight difference in the linear elastic behaviors of a single chain and star polymers. In the case of a single chain, the mean x component of the end-to-end vector $\langle x_N \rangle$ is rigorously equal to $R_0^2 X/3k_BT$, where $R_0^2 = \langle r_N^2 \rangle_0$ is the mean square end-to-end distance at $X = 0$. In contrast, the mean x component of the center-end vectors $\langle x_N^{(i)} \rangle$ of star polymers is not simply given by $R_0^2(M)X/3k_BT$, where $R_0^2(M) = \langle r_N^{(i)2} \rangle_0$ is the mean square center-end distance at $X = 0$. Instead, we show that the rigorous relation $\langle x_N^{(i)} \rangle / X = [R_0^2(M)/3 + (M - 1)\langle x_N^{(i)} x_N^{(j)} \rangle_0^{i \neq j}]/k_BT$ holds for small X, where $\langle x_N^{(i)} x_N^{(j)} \rangle_0^{i \neq j}$ denotes the mean product of the x components of the center-end vectors of the ith and jth arms in the absence of X. Here we perform large-scale Monte Carlo simulations of star self-avoiding walks (SAWs) on a simple cubic lattice with a lattice constant a. By using the enrichment algorithm generating 1 000 000 samples of star SAWs with $M = 2$, 3, 6 and 9 arms, each of which has the same chain length N up to 300, under the external force X, we find that the elastic behaviors of star polymers very much resemble those of a single chain obtained in our previous paper (*Macromolecules* 2008, *41*, 4037.), and are characterized as $\langle x_N^{(i)} \rangle \propto X$ (for very small X) and $\langle x_N^{(i)} \rangle \propto X^{2/3}$ (for $0 \ll X \sim k_BT/a$). The crossover between these two behaviors is smooth, and the crossover point is very much close to that of a single chain. Next, using the enrichment Monte Carlo simulation in the absence of the external force, we find that $R_0^2(M)$ is an increasing function of M and $\langle x_N^{(i)} x_N^{(j)} \rangle_0^{i \neq j}$ is a small negative quantity. This is consistent with our Monte Carlo result for the small X behavior of $\langle x_N^{(i)} \rangle / X$ that weakly decreases with increasing M. Also, by using a renormalization-group $\varepsilon = 4 - d$ expansion up to the first order in ϵ, we confirm that $\langle x_N^{(i)} x_N^{(j)} \rangle_0^{i \neq j}$ is a small negative quantity, whose small absolute value is independent of M and proportional to N. Finally, we briefly comment on the application of the present study to more general polymer networks.

I. Introduction

Star polymer is a simple polymer network composed of more than two flexible arm chains branching from a center unit. So far, dilute solutions of star polymers in good solvents have attracted fundamental interest both theoretically[1−20] and experimentally.[21−24] Their conformational properties,[1−6,21,22] entropic properties involving the total number of configurations,[5−12] osmotic pressures,[5,13−15,24] and dynamical properties[16−20,23] have been investigated and understood very well. However, elastic behaviors of star polymers have been examined neither theoretically nor experimentally, although there have been some theoretical attempts to treat elastic behaviors of polymer networks.[25−27] Recently, precise measurements of elastic behaviors of a single chain molecule have become possible by means of the atomic force microscopy (AFM),[28−31] and have stimulated theoretical studies of determining precise elastic behaviors of a flexible chain[32] and a semiflexible chain.[33,34]

On the other hand, the origin of rubber elasticity has been well understood in connection with entropic properties of flexible chains.[35] For a single flexible polymer chain composed of N segments (with segment length a) in a good solvents at temperature T, scaling theory,[35,36] Monte Carlo simulations,[32,37] and renormalization-group approach[38] have been used to determine its linear and nonlinear elastic behaviors: The mean x-component of the end-to-end vector $\langle x_N \rangle$ under an external force X exerted in the x direction behaves exactly as[32,35−38]

$$\langle x_N \rangle = \frac{1}{3}\beta X R_0^2, \quad \text{for } X \sim 0 \tag{1}$$

and as[32,35−38]

$$\langle x_N \rangle = \text{const.} \times X^{2/3}, \quad \text{for } 0 \ll X \sim k_BT/a \tag{2}$$

where $\beta = 1/k_BT$ and R_0^2 is the mean square end-to-end distance behaving as $\sim N^{2\nu}a$ with $\nu = 0.59$ as the exponent for the gyration radius.[35] In the case of a single chain, although there is no doubt in the validity of eqs 1 and 2, whether the transition between the linear (eq 1) and nonlinear (eq 2) elastic behaviors is abrupt or smooth has been a long standing problem until recently, although there were also some recent works.[39,40] In our recent Monte Carlo simulation,[32] which we will refer to as I, we found that the transition between these two behaviors is not an abrupt transition such as predicted by the previous Monte Carlo simulation[37] but a smooth crossover in accordance with the previous result of a renormalization-group analysis.[38]

In the present paper, we extend our previous study I on the linear and nonlinear elastic behaviors of a single flexible chain to the behaviors of M-arm star polymers. As well as I, we consider only good solvents. The purpose of this study is to clarify how the elastic behaviors of a single polymer chain and an M-arm star polymer are similar to or different from each other. As usual, we assume that each arm of an M-arm star polymer is made of a flexible polymer chain composed of N segments starting from a fixed center point O. We assume that the number of segments N is the same for every arm. We focus on the mean x-component of the center-end vectors $\langle x_N^{(i)} \rangle$ ($i = 1, ..., M$) under an external force X exerting on every end of the arms in the x direction. The main interest lies on the linear elastic behavior in the weak X regime and the crossover between the linear and nonlinear elastic behaviors in the intermediate X regime.

* Corresponding author. E-mail: ohno@ynu.ac.jp.

10.1021/ma801920p CCC: $40.75
Published on Web 03/30/2009

When X is small enough, it can be readily found that the exact relation

$$\langle x_N^{(i)}\rangle = \frac{\sum_{walks} x_N^{(i)} \exp(\beta X \sum_{k=1}^{M} x_N^{(k)})}{\sum_{walks} \exp(\beta X \sum_{k=1}^{M} x_N^{(k)})} \xrightarrow[X\to 0]{} \beta X \frac{\sum_{walks} x_N^{(i)} \sum_{k=1}^{M} x_N^{(k)}}{\sum_{walks} 1}$$
$$= \beta X \sum_{k=1}^{M} \langle x_N^{(i)} x_N^{(k)}\rangle_0$$
$$= \beta X(\langle x_N^{(i)2}\rangle_0 + (M-1)\langle x_N^{(i)} x_N^{(j)}\rangle_0^{i\neq j})$$
$$= \beta X\left(\frac{R_0{}^2(M)}{3} + (M-1)\langle x_N^{(i)} x_N^{(j)}\rangle_0^{i\neq j}\right) \quad (3)$$

holds in the limit $X\to 0$, where $R_0{}^2(M) = \langle x_N^{(i)2}\rangle_0 + \langle y_N^{(i)2}\rangle_0 + \langle z_N^{(i)2}\rangle_0 = \langle r_N^{(i)2}\rangle_0$ and $\langle x_N^{(i)} x_N^{(j)}\rangle_0^{i\neq j}$ are, respectively, the mean square center-end distance of the ith arm at $X = 0$ and the mean product of the x components of the center-end vectors of the ith and jth arms at $X = 0$. Here we used the indistinguishability of the arms and the spherical symmetry ($\langle x_N^{(i)2}\rangle_0 = \langle y_N^{(i)2}\rangle_0 = \langle z_N^{(i)2}\rangle_0$) of the end-point distribution of a star polymer in the absence of the external force. Note that eq 1 is a special case of $M = 1$ in eq 3. It is interesting to note that eq 3 holds for arbitrary strength of X in the case of Gaussian chains.[41] However, since $\langle x_N^{(i)}\rangle$ should not exceed Na even if the external force is large, eq 3 does not hold for large values of X. In fact, even for a simple N-step random walk, this relation is never satisfied for larger values of X as seen in section II.B of I.[32] For small X, eq 3, in principle, holds for individual arm of star. However, for numerical analysis, we take an average over all arms. According to Daoud and Cotton theory,[1] $R_0{}^2(M)$ is known to behave as

$$R_0{}^2(M) \approx M^{\sigma} N^{2\nu} \quad (4)$$

with $\sigma = 2(1-\nu)/(d-1) > 0$ for asymptotically large M,[1,10,11] where d is the spatial dimensionality. This $R_0{}^2(M)$ is an increasing function of the number M of arms due to the swollen (i.e., excluded volume) effect of the arm segments concentrated around the center point O. However, the elastic compliance (inverse of the elastic constant), which is equal to the mean x-component of the center-end vectors $\langle x_N^{(i)}\rangle$ divided by X, must be a decreasing function of M, because many other arms act as an obstacle around the center point O, preventing the ith arm to stretch in the x direction of the external force X. Why can the elastic compliance be a decreasing function of M in spite of the existence of an increasing function of $R_0{}^2(M)$ in eq 3? The only possible answer is that $\langle x_N^{(i)} x_N^{(j)}\rangle_0^{i\neq j}$ must be a negative quantity. Because the end points of the ith and jth arms repel each other, the center-end vector $\mathbf{r}_N^{(j)}$ of the jth arm has a tendency to point to the directions different from $\mathbf{r}_N^{(i)}$ of the ith arm, and the expectation value of the product of the x components of these two center-end vectors should certainly have a negative sign.

By means of a computer simulation of self-avoiding walks (SAWs) on a lattice, accurate analysis is possible,[42] and it is a straightforward application to study, for star SAWs, the linear and nonlinear elastic behaviors in the presence of the external force as well as the mean quantities, $R_0{}^2(M)$ and $\langle x_N^{(i)} x_N^{(j)}\rangle_0^{i\neq j}$, in the absence of the external force. Nevertheless, there have been only limited papers concerning such study on a single chain.[32,43,44] In the present paper, we will carry out a large-scale Monte Carlo simulation of M-arm star SAWs under a tensile force X exerting on the end points of the arms to analyze their linear and nonlinear elastic behaviors. By this simulation, we will find that the resulting behaviors are quite similar to those of a single chain obtained in I. Besides this similarity, we will also see that $\langle x_N^{(i)}\rangle/X$ at small X decreases weakly with increasing M as expected. According to the discussion given above in connection with eq 3, we will also investigate $R_0{}^2(M)$ and $\langle x_N^{(i)} x_N^{(j)}\rangle_0^{i\neq j}$ at $X = 0$ by using the same Monte Carlo simulation in the absence of the external force, and show that $\langle x_N^{(i)} x_N^{(j)}\rangle_0^{i\neq j}$ is a small negative quantity. Its absolute value is small and almost proportional to N, but decreases with increasing M. All these characteristics are consistent with each other via eq 3. For both these Monte Carlo simulations, we use the enrichment algorithm[10−13,15,18−20,32,45] to generate a lot of star SAW samples simultaneously. We generate 1 000 000 samples for each star SAW with up to $M = 9$ arms and $N = 300$ segments.

In addition to the Monte Carlo simulations, the renormalization-group (RG) calculations using the $\varepsilon = 4 - d$ expansion[5−8] can provide valuable information on the distribution functions of star polymers as well as the scaling theory.[1,3] In early 1980s, Miyake and Freed performed detailed calculations of the intersegment distance vectors and the radius of gyration of star polymers as well as the number of configurations up to the first order in ε.[5] The distribution functions involving center-end vectors can, however, be calculated more easily by using the magnetic spin analogy of the many-chain systems in the limit where the number of spin components n tends to zero.[6−8,35] Using this method, we will later show that the quantity $\langle x_N^{(i)} x_N^{(j)}\rangle_0^{i\neq j}$ is zero at the zeroth order in ϵ and has a negative contribution proportional to N and independent of M at the first order in ε.

The rest of this paper is organized as follows. In section II, the methodology of the enrichment Monte Carlo simulation is briefly described, and the results are presented in section III. The RG calculation is given in section IV. Finally, section V is devoted to summarize the main results of this paper, and there, we also give a brief comment on the relation to general polymer networks, which may be useful in the study of more complicated polymer networks.

II. Enrichment Monte Carlo Algorithm

In Monte Carlo simulations, it should be possible to calculate the center-end distribution function $f(r_N^{(k)})$ of a free star under zero external force to estimate $\langle x_N^{(k)}\rangle$ under the external force X by taking an average according to the distribution function multiplied by a Boltzmann factor $\exp(\beta X x_N^{(k)})$. However, the value of the distribution function $f(r_N^{(k)})$ is practically zero in the region $R_0 \ll r_N \sim Na$, because such a stretched-out configuration never occurs in the simple sampling method. The probability that such a configuration occurs is much smaller than the inverse of the total number of samples. Therefore, such a method cannot be used to calculate the force−distance curve in the strong force regime. This is the main reason why we use alternatively the importance sampling method.

In the present study, we use the enrichment algorithm[10−13,15,18−20,32,45] to elongate arms of star SAWs on a simple cubic lattice with lattice constant a. At the center of the star O, we assume a planar center unit in the yz plane at $x = 0$. Arms start from the different but mutually adjacent points around the origin on this planar unit. That is, the starting points of all the arms are located at $x = 0$ in the same yz plane. Their (y, z) coordinates are such that they are adjacent to each other. In this enrichment algorithm, we generate M arms with length $l + 1$ from those with length l by elongating simultaneously every end of the arms by Monte Carlo trials. On a simple cubic lattice, we have five ways of elongating one end of the arms by one segment, because the sixth direction makes the arm fold backward on itself. The probability of finding one sample in the enrichment algorithm is given by the product of the probability of choosing one direction at the lth elongation step

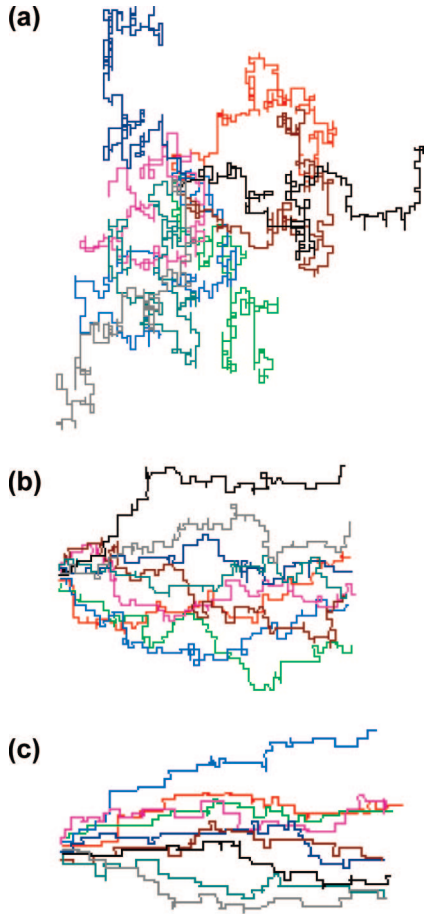

Figure 1. Typical configurations of 9-arm star SAWs generated by the enrichment Monte Carlo simulation with the external force, (a) $X = 0.05$, (b) $X = 1.0$, and (c) $X = 2.0$, acting in the right direction.

with respect to the number of segments, l, from $l = 1$ to $l = L$. The probability of finding any selected samples is equal to the number of the selected samples and the averaged probability of finding just one sample among many samples. This averaged probability of finding just one sample approaches the exact probability of finding one configuration out of all possible configurations as the number of samples increases. Therefore, the ensemble generated by the enrichment algorithm can well reproduce the ideal ensemble obtained by the exact enumeration using the direct counting method, when the number of samples is sufficiently large.

When the elongation starts at $x_0^{(k)} = 0$ as in the system treated in our paper, the relation

$$x_N^{(k)} = (x_1^{(k)} - x_0^{(k)}) + (x_2^{(k)} - x_1^{(k)}) + \ldots + (x_N^{(k)} - x_{N-1}^{(k)}) = \sum_{l=1}^{N} (x_l^{(k)} - x_{l-1}^{(k)}) \quad (5)$$

is always satisfied. Therefore we can replace the Boltzmann factor $\exp(\beta X x_N^{(k)})$ by

$$\exp[\beta X \sum_{l=1}^{N} (x_l^{(k)} - x_{l-1}^{(k)})] \quad (6)$$

for all arms k. This relation means that the system where only end points $x_N^{(k)}$ are pulled by the external force X is identical to the system where all segments $(x_l^{(k)} - x_{l-1}^{(k)})$ are pulled by the external force X. Indeed, the stars in the fluid flow, where all

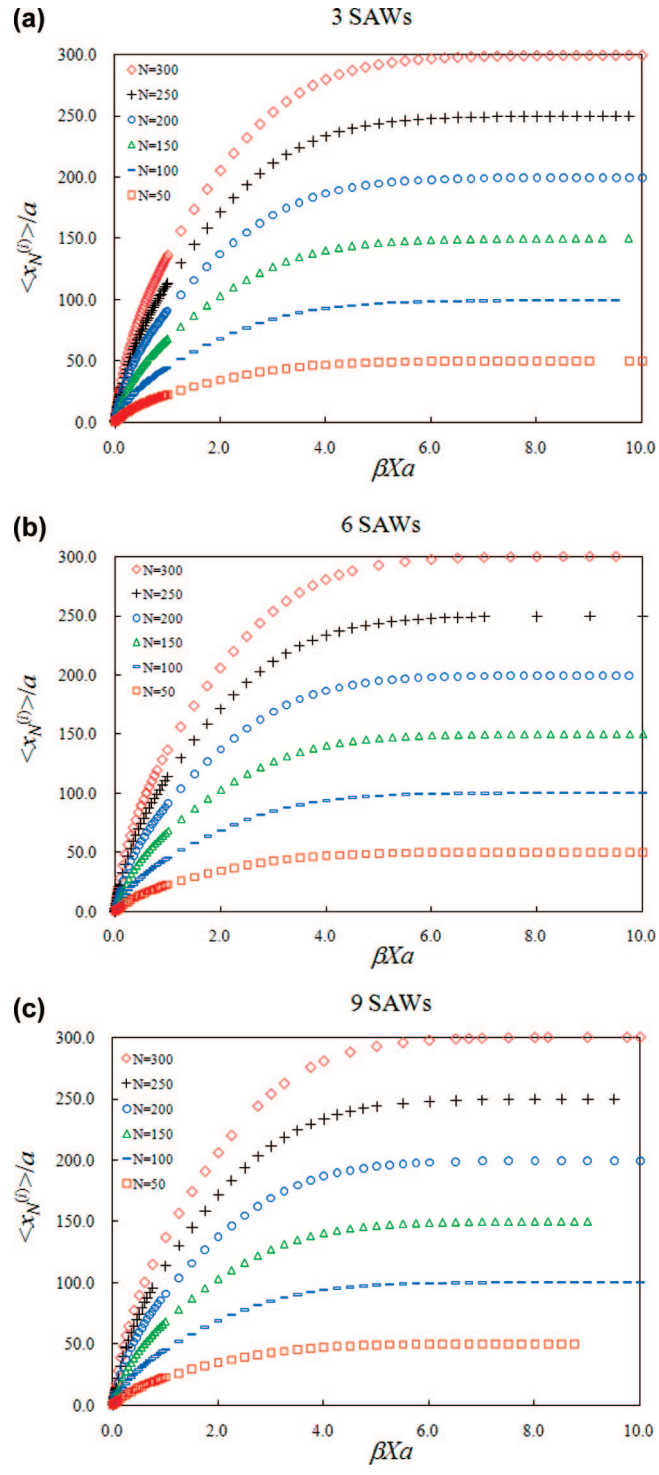

Figure 2. Force−distance curve obtained by the present Monte Carlo simulation. The mean x component of the center-end vectors $\langle x_N^{(i)} \rangle / a$ is plotted versus the external force X times βa for star polymers with (a) $M = 3$, (b) $M = 6$, and (c) $M = 9$ arms of length $N = 50$ (squares), 100 (bars), 150 (triangles), 200 (circles), 250 (crosses), and 300 (diamonds). The value $\langle x_N^{(i)} \rangle / a$ reaches N when X is large enough.

the arms are pulled in the direction of the fluid flow, behaves as if only end points are pulled in this direction. According to the importance-sampling method in the presence of the externals force X in the x direction, the probability of elongating one end depends on the direction of elongation and is given by

$$\frac{\exp[\beta X (x_l^{(k)} - x_{l-1}^{(k)})]}{e^{\beta X a} + e^{-\beta X a} + 4} \quad (7)$$

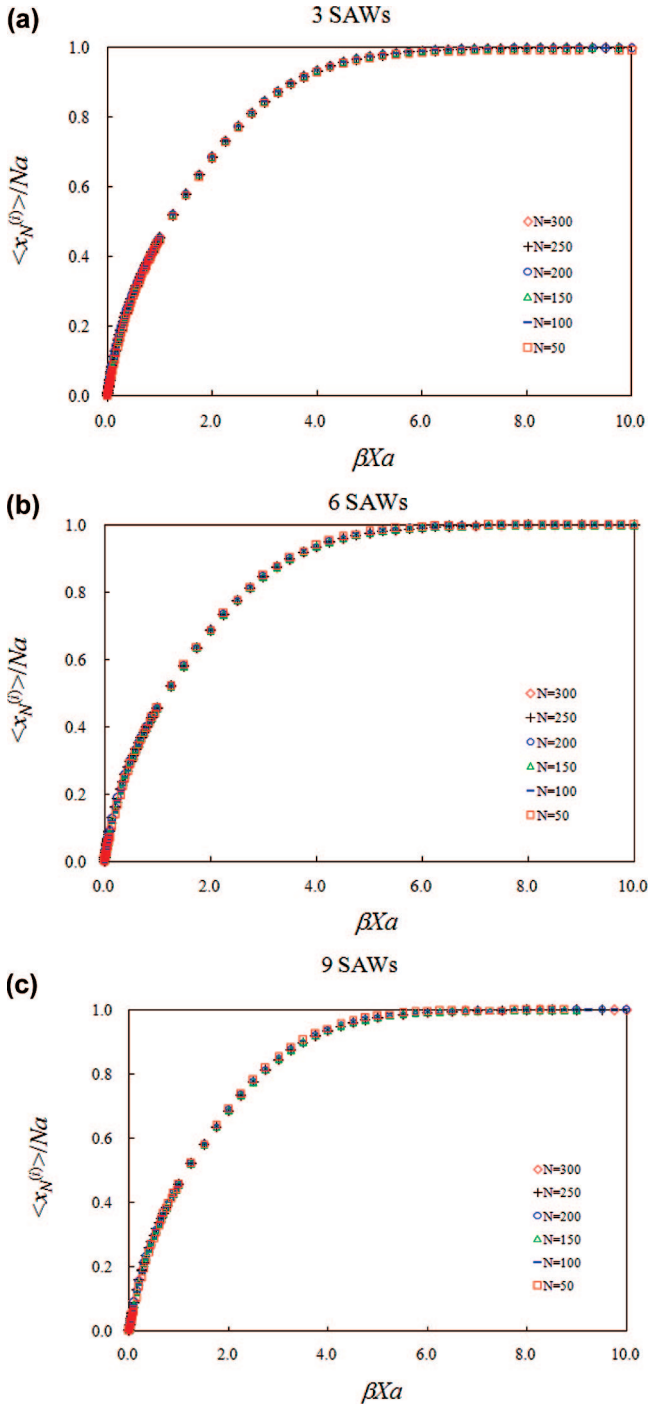

Figure 3. Replots of Figure 1 by normalizing the ordinate by the chain length N. The normalized values $\langle x_N^{(i)}\rangle/Na$ are plotted versus βXa for star polymers with (a) $M = 3$, (b) $M = 6$, and (c) $M = 9$ arms of length $N = 50$ (squares), 100 (bars), 150 (triangles), 200 (circles), 250 (crosses), and 300 (diamonds). In this plot, all the curves overlap very well onto a single curve.

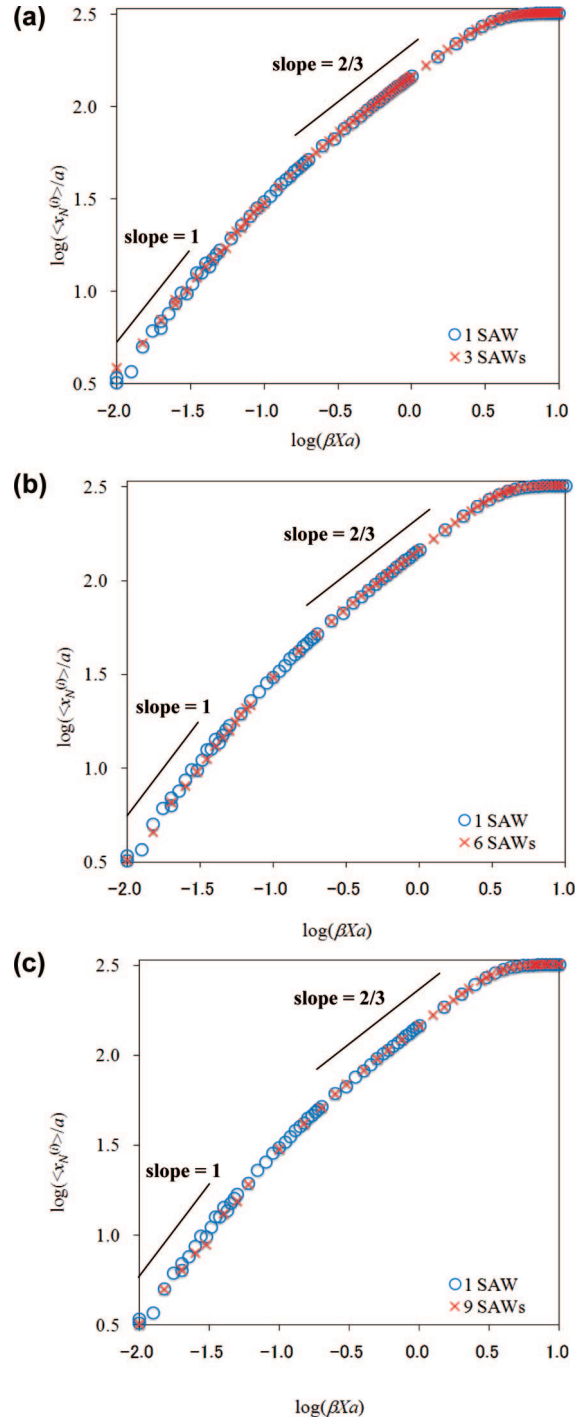

Figure 4. Double logarithmic plots of the force−distance curves of star polymers with (a) $M = 3$, (b) $M = 6$, and (c) $M = 9$ arms of length $N = 300$ (crosses) compared with the corresponding curve of a single chain of length $N = 300$ (circles). There is no visible difference between crosses and circles in (a) $M = 3$, whereas the crosses appear slightly lower than the circles in (b) $M = 6$ and (c) $M = 9$ in the linear elastic region for small X.

where the denominator is required for the normalization of the probability. Then, one-step larger stars are generated. At each step of this procedure, the self- and mutual-avoiding conditions are tested; unless the conditions are fulfilled, generated configurations are simply discarded. If there is no external force, the success ratio is asymptotically given by $\mu/5 = 0.93706$ (the effective coordination number of the simple cubic lattice is $\mu = 4.6853$[46]) for very long chains. Of course, the success ratio changes from this value when X is nonzero.

If we would consider all possible realizations at the $(l + 1)$st step from Φ_l distinct realizations at the lth step, we have to make all $5\Phi_l$ trials. However, doing only $m\Phi_l$ trials ($m < 5$) that are much less than the full $5\Phi_l$ trials, we can collect enough number of samples which are statistically isomorphic to the full realizations. That is, we generate only a limited number of samples Φ_{l+1} from Φ_l samples by a Monte Carlo method. This process can be iterated when $\Phi_l \sim \Phi_{l+1} \sim$ .... In practice, it is

Table 1. Crossover Point $\log(\beta X_c a)$, $\beta X_c a$, and the Corresponding $\eta_c = \beta X_c R_0(M)$ for Star Polymers with $M = 1, 2, 3, 6, 9$, and $N = 100, 200, 300$

	$M = 1$			$M = 2$			$M = 3$		
	$N = 100$	$N = 200$	$N = 300$	$N = 100$	$N = 200$	$N = 300$	$N = 100$	$N = 200$	$N = 300$
$\log(\beta X_c a)$	−0.69	−0.80	−1.04	−0.65	−0.79	−1.04	−0.65	−0.77	−1.04
$\beta X_c a$	0.205	0.158	0.091	0.225	0.163	0.091	0.225	0.171	0.091
$\eta_c = \beta X_c R_0(M)$	3.35	3.88	2.84	3.79	4.14	2.95	3.86	4.42	3.02

	$M = 6$			$M = 9$		
	$N = 100$	$N = 200$	$N = 300$	$N = 100$	$N = 200$	$N = 300$
$\log(\beta X_c a)$	−0.65	−0.77	−0.96	−0.64	−0.77	−0.92
$\beta X_c a$	0.226	0.171	0.110	0.228	0.170	0.120
$\eta_c = \beta X_c R_0(M)$	4.09	4.67	3.82	4.29	4.81	4.34

necessary to increase Φ_l gradually as l increases. This enrichment algorithm significantly reduces computing time, since it becomes quite efficient asymptotically for very long chains. In this way, we create 1 000 000 samples of star SAWs with number of arms M equal to 2, 3, 6, 9 and the length of each arm N equal to 100, 200, and 300 under various strengths of the external force X.

III. Numerical Results

First we present the results of our Monte Carlo simulation of star polymers under the external force X. Typical configurations of 9-arm star SAWs with length $N = 300$ generated by the enrichment Monte Carlo simulation with the external force, (a) $X = 0.05$, (b) $X = 1.0$, and (c) $X = 2.0$, are shown in Figure 1. The resulting mean x component of the center-end vectors $\langle x_N^{(i)}\rangle/a$ is plotted versus βXa for star polymers with $M = 3$, 6, and 9 arms and chain length $N = 50$, 100, 150, 200, 250 and 300 in Figure 2a−c. The estimation errors are so small that we do not show them in these figures. The value $\langle x_N^{(i)}\rangle/a$ increases linearly in X, and reaches N for large X, where all arms stretch in the x direction of the external force X. If we rescale the ordinate by the chain length N and superpose the results $\langle x_N^{(i)}\rangle/Na$ of all N in the same figure, all the curves for different chain lengths clearly overlap onto a single curve as seen in Figure 3a−c for 3-arm, 6-arm, and 9-arm star polymers. Moreover, comparing these figures, one may find that the behaviors of star polymers with different number of arms, M, are quite similar to each other. For the 3-arm, 6-arm, and 9-arm star polymers with the longest chain length $N = 300$, we replot the force−distance curves in double logarithmic scales in Figure 4a−c. There, we also plot the result of I for a single chain ($M = 1$) for comparison. From these figures, it is readily understood that the force−distance curve of star polymers is very close to that of a single chain. These results lead us to the conclusion that the elastic behavior of star polymers is surprisingly quite similar to that of a single chain. As in the case of a single chain, in the region of small X, $\log(\beta Xa) < -1.5$ (for $N = 300$), the slope is unity, i.e., the linear elastic behavior

$$\langle x_N^{(i)}\rangle = \text{const.} \times X, \quad \text{for } X \sim 0 \tag{8}$$

is maintained, while, in the region of medium X, $-0.7 < \log(\beta Xa) < 0.3$ (for $N = 300$), the slope is $^2/_3$, i.e., the nonlinear elastic behavior

$$\langle x_N^{(i)}\rangle = \text{const.} \times X^{2/3}, \quad \text{for } 0 \ll X \sim k_BT/a \tag{9}$$

is maintained. These two behaviors are the same as those we have confirmed in our previous study, I. Note that the latter region was written as $0 \ll X \ll k_BT/a$ in I according to des Gennes,[35] but eq 9 is actually satisfied even around the region $X \sim k_BT/a$ as seen in Figure 4. From this figure, one may find that the crossover between the linear and nonlinear elastic behaviors is smooth as well as a single chain. Whether the crossover is smooth or abrupt has been a long standing problem for a single chain. The smooth crossover was predicted in earlier renormalization-group calculation[37] and abrupt transition was observed in earlier Monte Carlo simulation with length $N =$ 10, 20, 40, and 80.[38] Our previous paper, I, together with the present paper, refutes the result of this earlier Monte Carlo study. The crossover point is located around $\log(\beta X_c a) = -1.04$ ($N =$ 300) to −0.64 ($N = 100$), and listed in Table 1. For given number of arms, M, the crossover point $\beta X_c a$ is found to be a monotonically decreasing function of N. On the other hand, at fixed N (=300), we find that the crossover point $\beta X_c a$ slightly increases as M increases, in particular, for large M. As seen also in Table 1, the critical value of $\eta = \beta XR_0(M)$, i.e., $\eta_c = \beta X_c R_0(M)$, is a clear increasing function of M at given N. The resulting value η_c may be compared with the result of the earlier renormalization-group calculation for a single chain ($M = 1$), which tells us that $\eta_c \sim 1$ irrespective of N.[37]

Besides the overall similarity, there is a subtle difference between the linear elastic behaviors of star polymers and of a single chain in the small X region. In the linear X region of Figure 4, parts b and c, the crosses of the 6-arm and 9-arm star polymers are located slightly lower than the circles of the linear chain (circles). Such a difference is, however, not seen in Figure 4a for the 3-arm star polymer. In parts a−c of Figure 5, the initial slope of $\langle x_N^{(i)}\rangle/a$ against βXa, i.e., $\langle x_N^{(i)}\rangle/\beta Xa^2$ for small X, is plotted (in circles) versus the number of arms, M, in double logarithmic scales, respectively, for (a) $N = 100$, (b) $N = 200$, and (c) $N = 300$. Although the estimation errors are large and $\langle x_N^{(i)}\rangle/\beta Xa^2$ does not show a clear dependence on M in part c, it slightly decreases with increasing M in parts a and b. This result suggests that the elastic compliance, $\langle x_N^{(i)}\rangle/X$, is a weakly decreasing function of M. This characteristic is no other than what we expect, because many other arms ($j \neq i$) act as an obstacle for the ith arm to stretch in the x direction. Eq 3 in Introduction shows that $\langle x_N^{(i)}\rangle/\beta X$ is not simply expressed by one-third of $R_0^2(M) = \langle r_N^{(i)2}\rangle_0$, which is an increasing function of M in accordance with eq 4, but compensated by $(M - 1) \times \langle x_N^{(i)} x_N^{(j)}\rangle_0^{i\neq j}$. It suggests that $\langle x_N^{(i)} x_N^{(j)}\rangle_0^{i\neq j}$ is a negative quantity.

To see the behavior of $\langle x_N^{(i)} x_N^{(j)}\rangle_0^{i\neq j}$ and $R_0^2(M) = \langle r_N^{(i)2}\rangle_0$, we have separately performed the Monte Carlo simulation of star polymers in the absence of the external force. The resulting values for these quantities are listed in Table 2 for all combinations of M and N. In the fourth column of this Table, the combination $R_0^2(M)/3 + (M - 1)\langle x_N^{(i)} x_N^{(j)}\rangle_0^{i\neq j}$ is also listed. This combination should be compared to $\langle x_N^{(i)}\rangle/\beta X$, which is estimated by the simulation with the external force X and given in the last column of this table. From this Table, we find that $R_0^2(M)$ is an increasing function of both M and N in accordance with eq 4 and that $\langle x_N^{(i)} x_N^{(j)}\rangle_0^{i\neq j}$ is negative. The absolute value of $\langle x_N^{(i)} x_N^{(j)}\rangle_0^{i\neq j}$ is small compared to $R_0^2(M)$, but increases with increasing N. We find that $R_0^2(M)$ behaves as eq 4 with $\nu = 0.590 \pm 0.001$ and $\sigma = 0.2 \pm 0.2$ (the former value, ν, is in very good agreement with the well-know value $\nu = 0.59$ for a single chain,[35] while the latter value, σ, is slightly smaller than

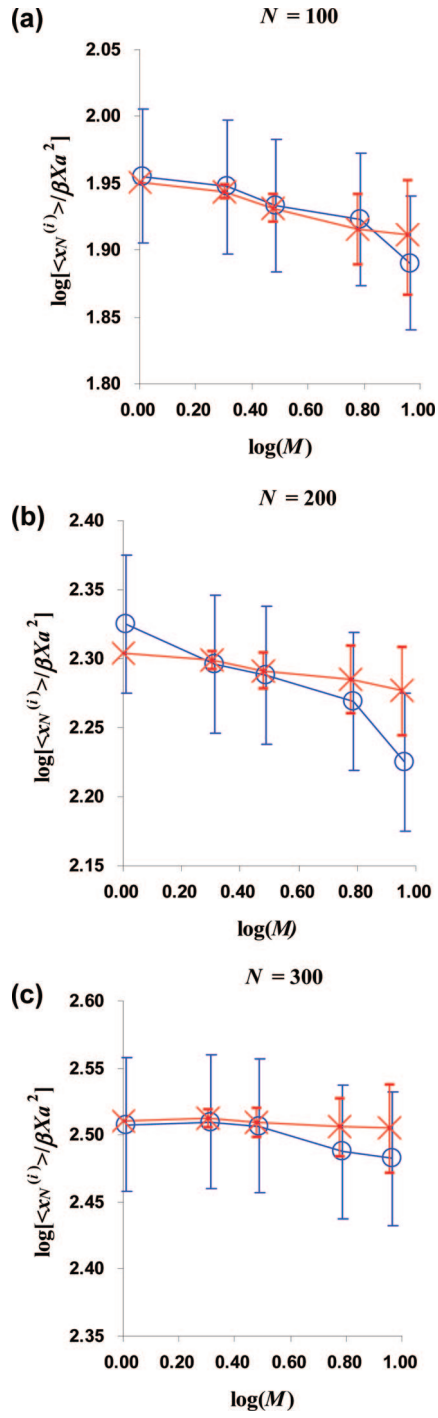

Figure 5. Double logarithmic plots of $\langle x_N^{(i)}\rangle/\beta X a^2$ derived from the simulations with small X (circles) and without X by using eq 3 (crosses) versus the number of arms, M. Figures (a), (b) and (c) are, respectively, for $N = 100$, $N = 200$, and $N = 300$. From this plot, one may suppose that $\langle x_N^{(i)}\rangle/\beta X a^2$ is a weakly decreasing function of M. See also Table 2.

$2(1 - \nu)/(d - 1) \approx 0.4$[1,11] because the number of arms M is not large enough in the present study), and $\langle x_N^{(i)} x_N^{(j)}\rangle_0^{i\neq j}$ behaves as

$$\langle x_N^{(i)} x_N^{(j)}\rangle_0^{i\neq j} \sim -M^{-\alpha} N^{\kappa} \tag{10}$$

with $\alpha = 0.2 \pm 0.2$ and $\kappa = 1.00 \pm 0.05$. The reason why $\langle x_N^{(i)} x_N^{(j)}\rangle_0^{i\neq j}$ is negative is that the end point of the jth arm has a tendency to point to directions different to the end point of the ith arm. In the next section, we will show that $\langle x_N^{(i)} x_N^{(j)}\rangle_0^{i\neq j}$ is a negative quantity by using the renormalization-group $\varepsilon = 4 - d$ expansion up to the first order in ε. The resulting combination $R_0^2(M)/3 + (M - 1)\langle x_N^{(i)} x_N^{(j)}\rangle_0^{i\neq j}$ in Table 2 very weakly decreases with increasing M, and is consistent with the result of Figure 5 for $\langle x_N^{(i)}\rangle/\beta X$. See also the crosses in Figure 5.

Table 2. Calculated Mean Product of x Components of Two End Vectors $\langle x_N^{(i)} x_N^{(j)}\rangle_0^{i\neq j}$, Mean Square Center-End Distance $R_0^2(M) = \langle r_N^{(i)2}\rangle_0$, and Their Combination[a] $\sum_{k=1}^{M}\langle x_N^{(i)} x_N^{(k)}\rangle_0 = R_0^2(M)/3 + (M - 1)\langle x_N^{(i)} x_N^{(j)}\rangle_0^{i\neq j}$ of a Star Polymer with M Arms, Each Composed of N Segments, in the Absence of the External Force X, in Units of a^2

N	$\langle x_N^{(i)} x_N^{(j)}\rangle_0^{i\neq j}/a^2$	$R_0^2(M)/a^2$	$R_0^2(M)/3a^2 + (M\text{-}1)\langle x_N^{(i)} x_N^{(j)}\rangle_0^{i\neq j}/a^2$	$\langle x_N^{(i)}\rangle/\beta X a^2$
		$M = 1$		
50		117	39	
100		268	89	90 ± 11
150		430	143	
200		604	201	212 ± 26
250		788	263	
300		973	324	313 ± 43
		$M = 2$		
50	−3 ± 1	125	38 ± 1	
100	−7 ± 1	285	88 ± 1	89 ± 10
150	−12 ± 2	456	140 ± 2	
200	−17 ± 3	648	199 ± 3	198 ± 22
250	−24 ± 5	835	254 ± 5	
300	−25 ± 5	1051	325 ± 5	318 ± 44
		$M = 3$		
50	−3 ± 1	131	38 ± 1	
100	−7 ± 1	297	85 ± 2	86 ± 10
150	−10 ± 2	481	140 ± 4	
200	−14 ± 3	669	195 ± 6	194 ± 23
250	−17 ± 3	882	260 ± 7	
300	−21 ± 4	1093	323 ± 8	317 ± 44
		$M = 6$		
50	−3 ± 1	147	36 ± 3	
100	−5 ± 1	328	82 ± 5	84 ± 10
150	−8 ± 2	532	138 ± 8	
200	−11 ± 2	749	193 ± 11	186 ± 23
250	−14 ± 3	984	256 ± 14	
300	−16 ± 3	1208	321 ± 16	304 ± 42
		$M = 9$		
50	−2 ± 1	158	35 ± 3	
100	−5 ± 1	354	81 ± 8	78 ± 9
150	−7 ± 1	569	130 ± 11	
200	−9 ± 2	796	189 ± 14	168 ± 20
250	−12 ± 2	1055	256 ± 19	
300	−15 ± 3	1311	320 ± 24	297 ± 41

[a] The last combination yields the elastic compliance $\langle x_N^{(i)}\rangle/\beta X$ for small X according to eq 3, which should be compared to the value in the last column estimated by the simulation with the external force X. For the comparison, see also Figure 5.

IV. Renormalization-Group Theory

Here, we start from the continuous S^4 model of a classical n-component spin system described by the Hamiltonian

$$H = \int \left[\frac{1}{2}\sum_{k=1}^{n}\{t_k S^{(k)2}(\mathbf{r}) + (\nabla S^{(k)}(\mathbf{r}))^2\} + \frac{u}{8}\Big(\sum_{k=1}^{n} S^{(k)2}(\mathbf{r})\Big)^2\right] \mathrm{d}\mathbf{r} \tag{11}$$

and invoke the magnetic spin analogy of many chain systems in the limit $n \to 0$.[35] The parameter t_k is related to the dimensionless exchange interaction $K_k = J_k/k_B T$ (J_k is the exchange interaction) between the kth components of nearest-neighbor spins of the original discrete n-vector spin model via the relation $K_k = K_c e^{-t_k}$ or $t_k \approx (K_c - K_k)/K_c$, where K_c denotes the critical point of the spin system and is given by $K_c = 1/\mu$, where μ is equal to the effective coordination number of a SAW. Then, one may find[6-8] that the total number of configurations of the star polymer with M arms starting at center points O_1, O_2,..., O_M (we assume these points

are adjacent to each other around the origin O) and ending at points P_1, P_2,..., P_M with arm lengths N_1, N_2,..., N_M, $Y(\mathbf{r}_{O_1}, \mathbf{r}_{O_2},..., \mathbf{r}_{O_M}; \mathbf{r}_{P_1}, \mathbf{r}_{P_2},..., \mathbf{r}_{P_M}; N_1, N_2,..., N_M)$, is related to the multispin correlation function as

$$\begin{aligned} &G(\mathbf{r}_{O_1}, \mathbf{r}_{O_2}, ..., \mathbf{r}_{O_M}; \mathbf{r}_{P_1}, \mathbf{r}_{P_2}, ..., \mathbf{r}_{P_M}; t_1, t_2, ..., t_M) \\ &= \langle \Phi_O^{(1,2,...,M)} S^{(1)}(\mathbf{r}_{P_1}) S^{(2)}(\mathbf{r}_{P_2}) \cdots S^{(M)}(\mathbf{r}_{P_M}) \rangle \\ &= \sum_{N_1} \sum_{N_2} \cdots \sum_{N_M} Y(\mathbf{r}_{O_1}, \mathbf{r}_{O_2}, ..., \mathbf{r}_{O_M}; \mathbf{r}_{P_1}, \mathbf{r}_{P_2}, ..., \mathbf{r}_{P_M}; \\ &\quad N_1, N_2, ..., N_M) K_1^{N_1} K_2^{N_2} \cdots K_M^{N_M} \\ &= \int_0^\infty \mathrm{d}N_1 \int_0^\infty \mathrm{d}N_2 \cdots \int_0^\infty \mathrm{d}N_M \times \\ &\quad \frac{Y(\mathbf{r}_{O_1}, \mathbf{r}_{O_2}, ..., \mathbf{r}_{O_M}; \mathbf{r}_{P_1}, \mathbf{r}_{P_2}, ..., \mathbf{r}_{P_M}; N_1, N_2, ..., N_M)}{\mu^{N_1+N_2+\cdots+N_M}} \times \\ &\quad \mathrm{e}^{-(t_1 N_1 + t_2 N_2 + \cdots + t_M N_M)} \end{aligned} \tag{12}$$

Here $\Phi_O^{(1,2,...,M)} = S^{(1)}(\mathbf{r}_{O_1}) S^{(2)}(\mathbf{r}_{O_2}) \cdots S^{(M)}(\mathbf{r}_{O_M})$ is the M-component composite operator. That is, the multispin correlation function $G(\mathbf{r}_{O_1}, \mathbf{r}_{O_2},..., \mathbf{r}_{O_M}; \mathbf{r}_{P_1}, \mathbf{r}_{P_2},..., \mathbf{r}_{P_M}; K)$ represents the multiple Laplace transformation of $Y(\mathbf{r}_{O_1}, \mathbf{r}_{O_2},..., \mathbf{r}_{O_M}; \mathbf{r}_{P_1}, \mathbf{r}_{P_2},..., \mathbf{r}_{P_M}; N_1, N_2,..., N_M)/\mu^{N_1+N_2+\cdots+N_M}$ of M arms starting at center O_i and ending at point P_i ($i = 1, 2,..., M$). In eq 12, the limit $n \to 0$ is taken for granted. Then, the mean product of x components of two different end vectors $\langle x_{N_i}^{(i)} x_{N_j}^{(j)} \rangle_0$ can be calculated as

$$\begin{aligned} \langle x_{N_i}^{(i)} x_{N_j}^{(j)} \rangle_0 = &\int \mathrm{d}\mathbf{r}_{P_1} \cdots \int x_{P_i} \mathrm{d}\mathbf{r}_{P_i} \cdots \int x_{P_j} \mathrm{d}\mathbf{r}_{P_j} \cdots \int \mathrm{d}\mathbf{r}_{P_M} \times \\ &Y(\mathbf{r}_{O_1}, ..., \mathbf{r}_{O_i}, ..., \mathbf{r}_{O_j}, ..., \mathbf{r}_{O_M}; \mathbf{r}_{P_1}, ..., \mathbf{r}_{P_i}, ..., \mathbf{r}_{P_j}, ..., \mathbf{r}_{P_M}; \\ &N_1, ..., N_i, ..., N_j, ..., N_M) / \int \mathrm{d}\mathbf{r}_{P_1} \cdots \int \mathrm{d}\mathbf{r}_{P_i} \cdots \int \mathrm{d}\mathbf{r}_{P_j} \cdots \\ &\int \mathrm{d}\mathbf{r}_{P_M} Y(\mathbf{r}_{O_1}, ..., \mathbf{r}_{O_i}, ..., \mathbf{r}_{O_j}, ..., \mathbf{r}_{O_M}; \mathbf{r}_{P_1}, ..., \mathbf{r}_{P_i}, ..., \\ &\mathbf{r}_{P_j}, ..., \mathbf{r}_{P_M}; N_1, ..., N_i, ..., N_j, ..., N_M) \\ = &\int \mathrm{d}\mathbf{r}_{P_1} \cdots \int x_{P_i} \mathrm{d}\mathbf{r}_{P_i} \cdots \int x_{P_j} \mathrm{d}\mathbf{r}_{P_j} \cdots \int \mathrm{d}\mathbf{r}_{P_M} \int_{c-i\infty}^{c+i\infty} \mathrm{d}t_1 \cdots \\ &\int_{c-i\infty}^{c+i\infty} \mathrm{d}t_i \cdots \int_{c-i\infty}^{c+i\infty} \mathrm{d}t_j \cdots \int_{c-i\infty}^{c+i\infty} \mathrm{d}t_M \, G(\mathbf{r}_{O_1}, ..., \mathbf{r}_{O_i}..., \mathbf{r}_{O_j}, ..., \mathbf{r}_{O_M}; \\ &\mathbf{r}_{P_1}, ..., \mathbf{r}_{P_i}..., \mathbf{r}_{P_j}, ..., \mathbf{r}_{P_M}; t_1, ..., t_i..., t_j, ..., t_M) \mathrm{e}^{(t_1 N_1 \cdots + t_i N_i \cdots + t_j N_j + \cdots + t_M N_M)} / \\ &\int \mathrm{d}\mathbf{r}_{P_1} \cdots \int \mathrm{d}\mathbf{r}_{P_i} \cdots \int \mathrm{d}\mathbf{r}_{P_j} \cdots \int \mathrm{d}\mathbf{r}_{P_M} \int_{c-i\infty}^{c+i\infty} \mathrm{d}t_1 \cdots \\ &\int_{c-i\infty}^{c+i\infty} \mathrm{d}t_i \cdots \int_{c-i\infty}^{c+i\infty} \mathrm{d}t_j \cdots \int_{c-i\infty}^{c+i\infty} \mathrm{d}t_M \, G(\mathbf{r}_{O_1}, ..., \mathbf{r}_{O_i}..., \mathbf{r}_{O_j}, ..., \mathbf{r}_{O_M}; \\ &\mathbf{r}_{P_1}, ..., \mathbf{r}_{P_i}..., \mathbf{r}_{P_j}, ..., \mathbf{r}_{P_M}; t_1, ..., t_i..., t_j, ..., t_M) \mathrm{e}^{(t_1 N_1 \cdots + t_i N_i \cdots + t_j N_j + \cdots + t_M N_M)} \end{aligned} \tag{13}$$

For the spatial dimension d greater than 4, fluctuations become negligible, and u in eq 11 can be omitted above the critical temperature, i.e., for $t > 0$. Then the Boltzmann distribution described by the Hamiltonian (eq 11) is a Gaussian distribution, and mean-field (decoupling) approximation is accurate:

$$\begin{aligned} &G(\mathbf{r}_{O_1}, \mathbf{r}_{O_2}, ..., \mathbf{r}_{O_M}; \mathbf{r}_{P_1}, \mathbf{r}_{P_2}, ..., \mathbf{r}_{P_M}; t_1, t_2, ..., t_M) = \\ &\quad g_{MF}(\mathbf{r}_{O_1}; \mathbf{r}_{P_1}; t_1) g_{MF}(\mathbf{r}_{O_2}; \mathbf{r}_{P_2}; t_2) \cdots g_{MF}(\mathbf{r}_{O_M}; \mathbf{r}_{P_M}; t_M), \quad \text{for } d > 4 \end{aligned} \tag{14}$$

where we introduced the mean-field propagator

$$g_{MF}(\mathbf{r}_{O_i}; \mathbf{r}_{P_i}; t_i) = \frac{1}{(2\pi)^d} \int \frac{\mathrm{e}^{i\mathbf{q}\cdot(\mathbf{r}_{P_i} - \mathbf{r}_{O_i})}}{t_i + q^2} \mathrm{d}\mathbf{q} \tag{15}$$

Since

$$\begin{aligned} \int g_{MF}(\mathbf{r}_{O_i}; \mathbf{r}_{P_i}; t_i) \, \mathrm{d}\mathbf{r}_{P_i} &= \frac{1}{(2\pi)^d} \int \frac{\mathrm{e}^{-i\mathbf{q}\mathbf{r}_{O_i}}}{t_i + q^2} \mathrm{d}\mathbf{q} \int \mathrm{e}^{i\mathbf{q}\mathbf{r}_{P_i}} \mathrm{d}\mathbf{r}_{P_i} \\ &= \int \frac{\mathrm{e}^{-i\mathbf{q}\mathbf{r}_{O_i}}}{t_i + q^2} \mathrm{d}\mathbf{q} \, \delta(\mathbf{q}) \\ &= \frac{1}{t_i}, \\ \int g_{MF}(\mathbf{r}_{O_i}; \mathbf{r}_{P_i}; t_i) x_{P_i} \, \mathrm{d}\mathbf{r}_{P_i} &= \frac{1}{(2\pi)^d} \int \frac{\mathrm{e}^{-i\mathbf{q}\mathbf{r}_{O_i}}}{t_i + q^2} \mathrm{d}\mathbf{q} \int \mathrm{e}^{i\mathbf{q}\mathbf{r}_{P_i}} x_{P_i} \, \mathrm{d}\mathbf{r}_{P_i} \\ &= -i \int \frac{\mathrm{e}^{-i\mathbf{q}\mathbf{r}_{O_i}}}{t_i + q^2} \mathrm{d}\mathbf{q} \frac{\partial}{\partial q_x} \delta(\mathbf{q}) \\ &= i \int \frac{\partial}{\partial q_x} \left(\frac{\mathrm{e}^{-i\mathbf{q}\mathbf{r}_{O_i}}}{t_i + q^2} \right) \mathrm{d}\mathbf{q} \, \delta(\mathbf{q}) \\ &= i \lim_{\mathbf{q}\to 0} \frac{\partial}{\partial q_x} \left(\frac{\mathrm{e}^{-i\mathbf{q}\mathbf{r}_{O_i}}}{t_i + q^2} \right) \\ &= \lim_{\mathbf{q}\to 0} \left(\frac{x_{O_i} \mathrm{e}^{-i\mathbf{q}\mathbf{r}_{O_i}}}{t_i + q^2} - \frac{2q_x \mathrm{e}^{-i\mathbf{q}\mathbf{r}_{O_i}}}{(t_i + q^2)^2} \right) \\ &= \frac{x_{O_i}}{t_i}, \\ \int g_{MF}(\mathbf{r}_{O_i}; \mathbf{r}_{P_i}; t_i) {r_{P_i}}^2 \, \mathrm{d}\mathbf{r}_{P_i} &= \frac{1}{(2\pi)^d} \int \frac{\mathrm{e}^{-i\mathbf{q}\mathbf{r}_{O_i}}}{t_i + q^2} \mathrm{d}\mathbf{q} \int \mathrm{e}^{i\mathbf{q}\mathbf{r}_{P_i}} {r_{P_i}}^2 \, \mathrm{d}\mathbf{r}_{P_i} \\ &= -\int \frac{\mathrm{e}^{-i\mathbf{q}\mathbf{r}_{O_i}}}{t_i + q^2} \mathrm{d}\mathbf{q} \, {\nabla_{\mathbf{q}}}^2 \delta(\mathbf{q}) \\ &= -\int {\nabla_{\mathbf{q}}}^2 \left(\frac{\mathrm{e}^{-i\mathbf{q}\mathbf{r}_{O_i}}}{t_i + q^2} \right) \mathrm{d}\mathbf{q} \, \delta(\mathbf{q}) \\ &= -\lim_{\mathbf{q}\to 0} {\nabla_{\mathbf{q}}}^2 \left(\frac{\mathrm{e}^{-i\mathbf{q}\mathbf{r}_{O_i}}}{t_i + q^2} \right) \\ &= \lim_{\mathbf{q}\to 0} \left(\frac{{r_{O_i}}^2 \mathrm{e}^{-i\mathbf{q}\mathbf{r}_{O_i}}}{t_i + q^2} - \frac{4i\mathbf{q}\mathbf{r}_{O_i} \mathrm{e}^{-i\mathbf{q}\mathbf{r}_{O_i}}}{(t_i + q^2)^2} - \right. \\ &\quad \left. \frac{8q^2 \mathrm{e}^{-i\mathbf{q}\mathbf{r}_{O_i}}}{(t_i + q^2)^3} + \frac{2d \mathrm{e}^{-i\mathbf{q}\mathbf{r}_{O_i}}}{(t_i + q^2)^2} \right) \\ &= \frac{{r_{O_i}}^2}{t_i} + \frac{2d}{t_i^2} \end{aligned} \tag{16}$$

eq 13 can be calculated as follows:

$$\begin{aligned} &\langle x_{N_i}^{(i)} x_{N_j}^{(j)} \rangle_0 = \\ &\quad x_{O_i} x_{O_j} \prod_{k=1}^{M} \int_{c-i\infty}^{c+i\infty} \frac{\mathrm{d}t_k}{t_k} \mathrm{e}^{t_k N_k} / \prod_{k=1}^{M} \int_{c-i\infty}^{c+i\infty} \frac{\mathrm{d}t_k}{t_k} \mathrm{e}^{t_k N_k} \xrightarrow[x_{O_i}, x_{O_j} \to 0]{} 0, \\ &\quad \langle r_N^{(i)^2} \rangle_0 = \int_{c-i\infty}^{c+i\infty} \mathrm{d}t_i \left(\frac{r_{O_i}^2}{t_i} + \frac{2d}{t_i^2} \right) \mathrm{e}^{t_i N_i} \prod_{\substack{j=1 \\ (j \neq i)}}^{M} \int_{c-i\infty}^{c+i\infty} \frac{\mathrm{d}t_k}{t_k} \mathrm{e}^{t_k N_k} / \\ &\qquad \prod_{k=1}^{M} \int_{c-i\infty}^{c+i\infty} \frac{\mathrm{d}t_k}{t_k} \mathrm{e}^{t_k N_k} \xrightarrow[r_{O_i} \to 0]{} 2dN_i, \quad \text{for } d > 4 \end{aligned} \tag{17}$$

where we used the elementary formulas of the inverse Laplace transformation

$$\int_{c-i\infty}^{c+i\infty} \frac{\mathrm{d}t_i}{t_i} \mathrm{e}^{t_i N_i} = 1, \quad \text{and} \quad \int_{c-i\infty}^{c+i\infty} \frac{\mathrm{d}t_i}{t_i^2} \mathrm{e}^{t_k N_k} = N_i \tag{18}$$

The first relation in eq 17, $\langle x_{N_r}^{(i)} x_{N_j}^{(j)} \rangle_0 = 0$, is obvious when no interaction exists among chains for $d > 4$, and the second

relation, $\langle r_N^{(i)2}\rangle_0 = 2dN$, is the well-known result of a random walk (RW) not interacting with other chains.

On the other hand, for the spatial dimensionality d slightly less than 4, one may regard u as a weak perturbation, using the renormalization-group $\epsilon = 4 - d$ expansion. To the first order in ϵ, there is only one diagram relevant to $\langle x_{N_i}^{(i)} x_{N_j}^{(j)}\rangle_0$. It is shown in Figure 6, where the straight lines denote $g_{MF}(\mathbf{r};\mathbf{r}';t_k)$ with $k = i$ or j, and the dotted line represents u. This diagram can be evaluated as follows:

$$
\begin{aligned}
-u \int g_{MF}(0;\mathbf{r};t_i) g_{MF}(0;\mathbf{r};t_j)\, \mathrm{d}\mathbf{r} \int g_{MF}(\mathbf{r};\mathbf{r}_{P_i};t_i) x_{P_i}\, \mathrm{d}\mathbf{r}_{P_i} \times \\
\int g_{MF}(\mathbf{r};\mathbf{r}_{P_j};t_j) x_{P_j}\, \mathrm{d}\mathbf{r}_{P_j} = -\frac{u}{t_i t_j} \int g_{MF}(0;\mathbf{r};t_i) g_{MF}(0;\mathbf{r};t_j) x^2\, \mathrm{d}\mathbf{r} \\
= \frac{1}{3 t_i t_j} \int g_{MF}(0;\mathbf{r};t_i) g_{MF}(0;\mathbf{r};t_j) r^2\, \mathrm{d}\mathbf{r} \\
= -\frac{u}{3 t_i t_j} \frac{1}{(2\pi)^{2d}} \int \frac{1}{(t_i + q_1^{\,2})(t_j + q_2^{\,2})}\, \mathrm{d}\mathbf{q}_1\, \mathrm{d}\mathbf{q}_2 \\
\int \mathrm{e}^{i(\mathbf{q}_1 + \mathbf{q}_2)\cdot\mathbf{r}} r^2\, \mathrm{d}\mathbf{r} \\
= \frac{8u}{3 t_i t_j} \frac{1}{(2\pi)^d} \int \frac{1}{[4t_i + (\mathbf{q}_+ + \mathbf{q}_-)^2][4t_j + (\mathbf{q}_+ - \mathbf{q}_-)^2]} \times \\
\mathrm{d}\mathbf{q}_+\, \mathrm{d}\mathbf{q}_- \nabla_{\mathbf{q}_+}^{\,2} \delta(\mathbf{q}_+) = \frac{8u}{3 t_i t_j} \frac{1}{(2\pi)^d} \times \\
\int \nabla_{\mathbf{q}_+}^{\,2} \left(\frac{1}{[4t_i + (\mathbf{q}_+ + \mathbf{q}_-)^2][4t_j + (\mathbf{q}_+ - \mathbf{q}_-)^2]} \right) \times \\
\mathrm{d}\mathbf{q}_+\, \mathrm{d}\mathbf{q}_- \delta(\mathbf{q}_+) \quad (19)
\end{aligned}
$$

where we put $\mathbf{q}_+ = \mathbf{q}_1 + \mathbf{q}_2$ and $\mathbf{q}_- = \mathbf{q}_1 - \mathbf{q}_2$. After some lengthy algebra, it is identified to be

$$
-\frac{8u}{3} \frac{\Omega_d}{(2\pi)^d} \left[\frac{8}{t_j (t_i - t_j)^2} + \frac{8}{t_i (t_i - t_j)^2} + \frac{4 - d}{t_i t_j (t_j - t_i)} \log \left| \frac{t_i}{t_j} \right| + \frac{16}{(t_j - t_i)^3} \log \left| \frac{t_i}{t_j} \right| \right] \quad (20)
$$

where we used the surface area of d-dimensional unit hypersphere, $\Omega_d = 2\pi^{d/2}/\Gamma(d/2)$, where Γ is the gamma function. Then we find

$$
\begin{aligned}
\langle x_{N_i}^{(i)} x_{N_j}^{(j)}\rangle_0 = -\frac{8u}{3} \frac{\Omega_d}{(2\pi)^d} \int_{c-i\infty}^{c+i\infty} \mathrm{d}t_i\, \mathrm{e}^{t_i N_i} \int_{c-i\infty}^{c+i\infty} \mathrm{d}t_j\, \mathrm{e}^{t_j N_j} \times \\
\left[\frac{8}{t_j (t_i - t_j)^2} + \frac{8}{t_i (t_i - t_j)^2} + \frac{4 - d}{t_i t_j (t_j - t_i)} \log \left| \frac{t_i}{t_j} \right| \right] - \\
\frac{8u}{3} \frac{\Omega_d}{(2\pi)^d} \int_{c-i\infty}^{c+i\infty} \mathrm{d}t_i\, \mathrm{e}^{t_i N_i} \int_{c-i\infty}^{c+i\infty} \mathrm{d}t_j\, \mathrm{e}^{t_j N_j} \frac{16}{(t_j - t_i)^3} \log \left| \frac{t_i}{t_j} \right| \\
= -\frac{8u}{3} \frac{\Omega_d}{(2\pi)^d} [8(N_i + N_j) - 2(4 - d)(N_i + N_j) \log |N_i + N_j| + \\
(4 - d)(N_i \log |N_i| + N_j \log |N_j|)] \xrightarrow[d \to 4]{} -\frac{8u}{3} \frac{\Omega_d}{(2\pi)^d} 8(N_i + N_j)
\end{aligned} \quad (21)
$$

From eqs 17 and 21 with the fixed point value $u^* = (4\pi)^{d/2}\varepsilon/(n + 8)$ for u[6−8,35] and $n = 0$, we find that $\langle x_{N_i}^{(i)} x_{N_j}^{(j)}\rangle_0$ is zero at the lowest (zeroth) order in ϵ and has a negative correction proportional to the sum of the two chain lengths $N_i + N_j$ at the first order in ϵ. That is, to the first order in ϵ, $\langle x_N^{(i)} x_N^{(j)}\rangle_0$ is a negative quantity proportional to N and independent of M. This behavior is certainly consistent what we observed in our Monte Carlo simulations. We do not know, however, whether there is a fractal power dependence on N and M even if the fractional part of the associated exponents is a small number. To explore the existence of such fractional power dependence, it is necessary to go beyond the first order calculation and to carry out the second order calculation. Such a calculation is, however, beyond the scope of the present analysis and left for a future study.

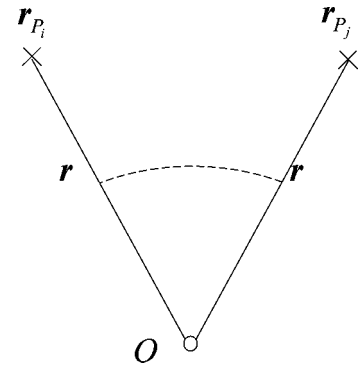

Figure 6. Relevant diagram contributing to $\langle x_{N_i}^{(i)} x_{N_j}^{(j)}\rangle_0$ at the first order in ϵ. This diagram can be evaluated as eq 19.

V. Summary and Relation to More General Polymer Networks

In this paper, we have investigated the elastic behaviors of star polymers. In particular, we have carried out large-scale Monte Carlo simulation of star polymers under an external force by means of the enrichment algorithm generating 1 000 000 samples of star SAWs with up to $M = 9$ arms each of which has chain length N up to $N = 300$. We have found that the elastic behaviors of star polymers are quite similar to those of a single chain and confirmed that nonlinear behavior proportional to $X^{2/3}$ (eq 9) appears in the region $0 \ll X \sim k_B T/a$. The crossover between the linear (eq 8) and nonlinear (eq 9) elastic behaviors of star polymers is smooth as well as the case of a single chain. This together with the result of our previous paper I on a single chain[32] refutes the abrupt transition reported in earlier Monte Carlo study on a relatively short single chain.[38] As shown in Table 1, the crossover point $\beta X_c a$ is very weakly increases with increasing M. There is a subtle difference in the linear elastic behavior in the region of small X. Our enrichment Monte Carlo result shows that the elastic compliance, $\langle x_N^{(i)}\rangle/X$, is a weakly decreasing function of M, although $R_0^2(M) = \langle r_N^{(i)2}\rangle_0$ is an increasing function of M in accordance with eq 4. For a single chain, the relation $\langle x_N\rangle = \beta X R_0^2/3$ (eq 1) holds rigorously, while, for an M-arm star polymer, $\langle x_N^{(i)}\rangle/\beta X$ is not simply expressed by one-third of $R_0^2(M)$, but compensated by $(M - 1)\langle x_N^{(i)} x_N^{(j)}\rangle_0^{i\neq j}$; see eq 3. By carrying out separately a Monte Carlo simulation in the absence of the external field, we found that $\langle x_N^{(i)} x_N^{(j)}\rangle_0^{i\neq j}$ is a small negative quantity, whose small absolute value is proportional to $M^{-\alpha} N^{\kappa}$ with $\alpha = 0.2 \pm 0.2$ and $\kappa = 1.00 \pm 0.05$. We also performed the renormalization-group $\epsilon = 4 - d$ expansion, and found that $\langle x_N^{(i)} x_N^{(j)}\rangle_0^{i\neq j}$ is a small negative quantity linearly proportional to N and independent of M up to the first order in ϵ.

Finally, we will make a brief comment on the application of the present theory to more general polymer networks. The star polymers studied in this paper may provide a prototype example of general polymer networks. In particular, eq 3 is a general identity and applicable to more complicated polymer networks with just a slight modification. In general cases, one may consider the system where some points of the polymer network are spatially fixed and the external force X is exerted in the x direction on some of the other points of the network. The number M denotes the number of points to which the external force X is applied. The most important and universal part of eq

3 is that it relates the elastic compliance of the polymer network to the sum of the mean products of the x coordinates of arbitrary two points among the M points to which external force X is applied, i.e., the correlation functions between two points of the network $\langle x_N^{(i)} x_N^{(j)} \rangle_0$, in the absence of the external force X. The rigorous relation for general polymer networks is expressed as

$$\langle x_N^{(i)} \rangle - \langle x_N^{(i)} \rangle_0 \xrightarrow[X \to 0]{} \beta X \sum_{j=1}^{M} (\langle x_N^{(i)} x_N^{(j)} \rangle_0 - \langle x_N^{(i)} \rangle_0 \langle x_N^{(j)} \rangle_0) = \beta X (\langle x_N^{(i)2} \rangle_0 - \langle x_N^{(i)} \rangle_0^2) + \sum_{\substack{j=1 \\ (j \neq i)}}^{M} (\langle x_N^{(i)} x_N^{(j)} \rangle_0^{i \neq j} - \langle x_N^{(i)} \rangle_0 \langle x_N^{(j)} \rangle_0)) \tag{22}$$

This relation relates the mean elongation $\langle x_N^{(i)} \rangle - \langle x_N^{(i)} \rangle_0$ under the external force X to the two-point correlation functions $\langle x_N^{(i)} x_N^{(j)} \rangle_0 - \langle x_N^{(i)} \rangle_0 \langle x_N^{(j)} \rangle_0$ in the absence of the external force. It would make the investigation of the elastic compliance $\langle x_N^{(i)} \rangle / X$ of complicated polymer networks, e.g. the analyses such as the renormalization-group approach, significantly much tractable. In this case, however, the repulsion between two points $\mathbf{r}_N^{(i)}$ and $\mathbf{r}_N^{(j)}$ due to the excluded volume effect will not necessary make the value $\langle x_N^{(i)} x_N^{(j)} \rangle_0^{i \neq j}$ negative but will depend on the architecture of the network such as the information whether the two points are relatively near or far each other in the structure of the network.

In this paper, since our main interest lies in the description of the rubber elasticity of the bundle of polymers, we have not considered an experimental situation that one of the arms (say, first arm) is fixed at the position $x_0 = 0$ and one of the other arms (say second arm) is pulled by the external force X (and all the other arms are free). However, when the external force X is weak, this situation can be described by eq 22. Indeed, in this case, eq 22 becomes just

$$\langle x_N^{(2)} \rangle = \xrightarrow[X \to 0]{} \beta X \langle (x_N^{(2)})^2 \rangle_0 = \frac{\beta X}{3} \langle (r_N^{(2)})^2 \rangle_0 \tag{23}$$

Here $\langle (r_N^{(2)})^2 \rangle_0$ is the mean square end-to-end distance of the star, which has been analyzed in a lot of earlier numerical analysis including Monte Carlo and molecular dynamics simulations of star polymers.

We can also consider different situations, where M_1 arms are fixed and the other M_2 ($=M - M_1$) arms are pulled, or equivalently, M_1 arms are pulled left and M_2 arms are pulled right. Obviously, the resulting configuration becomes such that M_1-arm star spreads leftward and M_2-arm star spreads rightward. Under a large external force X, M_1-arm star and M_2-arm star do not overlap, and behave independent stars. If the strength of the external force is relatively small, the force−distance behavior of this star can be again described by the exact relation eq 22. Therefore, anyway, the behavior of different situations can be described within the scope of our paper. So, we believe that eq 22 is the most fundamental result, which can be applied to not only different pulling conditions of star polymers like these examples but also any arbitrary polymer networks.

Acknowledgment. The authors acknowledge the use of the HITACHI SR11000 supercomputer at the Information Initiative Center of Hokkaido University. This work has been partly supported by the Grant-in-Aid for Scientific Research in Priority Areas (Grant No. 19019005) from the Ministry of Education, Culture, Sports, Science and Technology of Japan.

References and Notes

(1) Daoud, M.; Cotton, J. P. *J. Phys. (Paris)* **1982**, *43*, 531.
(2) Grest, G. S.; Kremer, K.; Witten, T. A. *Macromolecules* **1987**, *20*, 1376.
(3) Ohno, K.; Binder, K. *J. Chem. Phys.* **1991**, *95*, 5444 and 5459.
(4) Freire, J. J. *Adv. Polym. Sci.* **1999**, *143*, 35.
(5) Miyake, A.; Freed, K. F. *Macromolecules* **1983**, *16*, 1228.
(6) Ohno, K.; Binder, K. *J. Phys. (Paris)* **1988**, *49*, 1329.
(7) Ohno, K. *Phys. Rev. A* **1989**, *40*, 1524.
(8) von Ferber, C. *Condens. Matter Phys.* **2002**, *5*, 117. http://www.icmp.lviv.ua/journal/zbirnyk.29/index.html.
(9) Batoulis, J.; Kremer, K. *Macromolecules* **1989**, *22*, 4277.
(10) Ohno, K.; Binder, K. *J. Stat. Phys.* **1991**, *64*, 781.
(11) Ohno, K. *Macromol. Symp.* **1994**, *81*, 121.
(12) Ohno, K. *Condensed Matter Physics* **2002**, *5*, 15. http://www.icmp.lviv.ua/journal/zbirnyk.29/index.html.
(13) Ohno, K.; Shida, K.; Kimura, M.; Kawazoe, Y. *Macromolecules* **1996**, *29*, 2269.
(14) Rubio, A.; Freire, J. J. *Macromolecules* **1996**, *29*, 6946.
(15) Shida, K.; Ohno, K.; Kawazoe, Y.; Nakamura, Y. *J. Chem. Phys.* **2002**, *117*, 9942.
(16) Wilkinson, M. K.; Gaunt, D. S.; Lipson, J. E. G.; Whittington, S. G. *Macromolecules* **1988**, *21*, 1818.
(17) Grest, G. S.; Kremer, K.; Milner, S. T.; Witten, T. A. *Macromolecules* **1989**, *22*, 1904.
(18) Ohno, K.; Schultz, K.; Binder, K.; Frisch, H. L. *J. Chem. Phys.* **1994**, *101*, 4452.
(19) Shida, K.; Ohno, K.; Kimura, M.; Kawazoe, Y.; Nakamura, Y. *Macromolecules* **1998**, *31*, 2343.
(20) Shida, K.; Ohno, K.; Kawazoe, Y.; Nakamura, Y. *Polymer* **2004**, *45*, 1729.
(21) Roovers, J.; Hadjichristidis, N.; Fetters, L. J. *Macromolecules* **1983**, *16*, 214.
(22) Khasat, N.; Pennisi, R. W.; Hadjichristidis, N.; Fetters, L. J. *Macromolecules* **1988**, *21*, 1100.
(23) Roovers, J. *Macromolecules* **1994**, *27*, 5259.
(24) Okumoto, M.; Nakamura, Y.; Norisue, T.; Teramoto, A. *Macromolecules* **1998**, *31*, 1615.
(25) Everaers, R.; Kremer, K. *Macromolecules* **1995**, *28*, 7291.
(26) Cifra, P.; Bleha, T. *Macromolecules* **1998**, *31*, 1358.
(27) Rottach, D. R.; Curro, J. G.; Vudzien, J.; Grest, G. S.; Svaneborg, C.; Everaers, R. *Macromolecules* **2006**, *39*, 5521.
(28) Maaloum, M.; Courvoisier, A. *Macromolecules* **1999**, *32*, 4989.
(29) Hugel, T.; Grosholz, M.; Clausen-Schaumann, H.; Pfau, A.; Gaub, H.; Seitz, M. *Macromolecules* **2001**, *34*, 1039.
(30) Watabe, H.; Nakajima, K.; Sakai, Y.; Nishi, T. *Macromolecules* **2006**, *39*, 5921.
(31) Duschner, S.; Gröhn, F.; Maskos, M. *Polymer* **2006**, *47*, 7391.
(32) Masatsuji, S.; Nakagawa, N.; Ohno, K. *Macromolecules* **2008**, *41*, 4037.
(33) Rosa, A.; Hang, T. X.; Marenduzzo, D.; Martin, A. *Macromolecules* **2003**, *36*, 10095.
(34) Cifra, P.; Bleha, T. *Polymer* **2007**, *48*, 2444.
(35) de Gennes, P. *Scaling Concepts in Polymer Physics*; Cornell University Press: Ithaca, NY, 1979.
(36) Pincus, P. *Macromolecules* **1976**, *9*, 386.
(37) Oono, Y.; Ohta, T.; Freed, K. F. *Macromolecules* **1981**, *14*, 880.
(38) Webman, I.; Lebowitz, J. L.; Kalos, M. H. *Phys. Rev. A* **1981**, *23*, 316.
(39) Lam, P.-M. *Biopolymers* **2002**, *64*, 57.
(40) Toan, N. M.; Marenduzzo, D.; Micheletti, C. *Biophys. J.* **2005**, *89*, 80.
(41) Flory, P. J. *Statistical Mechanics of Chain Molecules*; Interscience; New York, 1969.
(42) Sokal, A. D.In *Monte Carlo and Molecular Dynamics Simulations in Polymer Science*; Binder, K., Ed.; Oxford University Press: Oxford, U.K., 1995.
(43) Wittkop, M.; Sommer, J.-U.; Kreitmeier, S.; Göritz, D. *Phys. Rev. E* **1994**, *49*, 5472.
(44) Cifra, P.; Bleha, T. *Macromol. Theory Simul.* **1995**, *4*, 233.
(45) Ohno, K.; Sakamoto, T.; Minagawa, T.; Okabe, Y. *Macromolecules* **2007**, *40*, 723.
(46) Watts, M. J. *J. Phys. A* **1975**, *8*, 61.

MA801920P